AMERICAN SOCIETY FOR MICROBIOLOGY | Antimicrobial Agents and Chemotherapy®

EXPERIMENTAL THERAPEUTICS

Antimicrobial and Antibiofilm Efficacy of Graphene Oxide against Chronic Wound Microorganisms

Mara Di Giulio,[a] Romina Zappacosta,[a] Silvia Di Lodovico,[a] Emanuela Di Campli,[a] Gabriella Siani,[a] Antonella Fontana,[a] Luigina Cellini[a]

[a]Department of Pharmacy, University "G. d'Annunzio" Chieti-Pescara, Chieti, Italy

ABSTRACT Chronic wounds represent an increasing problem worldwide. Graphene oxide (GO) has been reported to exhibit strong antibacterial activity toward both Gram-positive and Gram-negative bacteria. The aim of this work was to investigate the *in vitro* antimicrobial and antibiofilm efficacy of GO against wound pathogens. *Staphylococcus aureus* PECHA 10, *Pseudomonas aeruginosa* PECHA 4, and *Candida albicans* X3 clinical isolates were incubated with 50 mg/liter of GO for 2 and 24 h to evaluate the antimicrobial effect. Optical and atomic force microscopy images were performed to visualize the effect of GO on microbial cells. Moreover, the antibiofilm effect of GO was tested on biofilms, both in formation and mature. Compared to the respective time controls, GO significantly reduced the *S. aureus* growth both at 2 and 24 h in a time-dependent way, and it displayed a bacteriostatic effect in respect to the GO $t = 0$; an immediate (after 2 h) slowdown of bacterial growth was detected for *P. aeruginosa*, whereas a tardive effect (after 24 h) was recorded for *C. albicans*. Atomic force microscopy images showed the complete wrapping of *S. aureus* and *C. albicans* with GO sheets, which explains its antimicrobial activity. Moreover, significant inhibition of biofilm formation and a reduction of mature biofilm were recorded for each detected microorganism. The antibacterial and antibiofilm properties of GO against chronic wound microorganisms make it an interesting candidate to incorporate into wound bandages to treat and/or prevent microbial infections.

KEYWORDS chronic wound microorganisms, graphene oxide, antibacterial activity, antibiofilm activity

Chronic wounds represent an increasing problem worldwide and are difficult to heal, becoming an important challenge for the health care system (1). Chronic wounds, such as diabetic foot ulcers, venous ulcers, and surgical nonhealing wounds, cause poor quality of life and discomfort in patients, in addition to high health care costs (2). It is known that chronic wounds exhibit prolonged inflammation and persistent microbial infections, and multispecies drug-resistant microbial biofilms are often present (3, 4).

Staphylococcus aureus and *Pseudomonas aeruginosa* are the most prevalent bacteria isolated from wounds and are frequently found together, forming mixed clusters; *S. aureus* is located on the wound surface, whereas *P. aeruginosa* is in the deeper region of the chronic wound bed (5, 6). Also, the opportunistic pathogen *Candida albicans* is known to be associated with the mixed microbiota of wounds, and it contributes to formation of a dense synergistic complex with bacteria (7, 8).

A number of studies have shown the presence of microbial biofilms in chronic wounds. Biofilms represent an important challenge in infectious diseases, due to difficulty in treatment that interferes seriously with healing processes (6).

The antibiotic tolerance of microbial biofilm, together with the presence of drug-resistant strains, make the eradication of bacteria difficult, mainly due to the limited

Received 19 March 2018 **Returned for modification** 9 April 2018

Accepted manuscript posted online 16 April 2018

Citation Di Giulio M, Zappacosta R, Di Lodovico S, Di Campli E, Siani G, Fontana A, Cellini L. 2018. Antimicrobial and antibiofilm efficacy of graphene oxide against chronic wound microorganisms. Antimicrob Agents Chemother 62:e00547-18. https://doi.org/10.1128/AAC.00547-18.

Address correspondence to Mara Di Giulio, mara.digiulio@unich.it.

penetration of antibiotics or their ineffectiveness against resistant strains (9). For these reasons, new strategies should be conceived in order to treat chronic wounds.

Graphene has emerged in the last 15 years as an exceptional material that is able to conduct electrons and heat and that possess an extremely high mechanical strength associated with a high elasticity. These properties are enclosed in a two-dimensional (2D) material with a very high aspect ratio and therefore a low weight/superficial area value (10). All of these features, gathered in one material, confer on graphene characteristics of high interest for meaningful applications. Graphene has therefore been exploited in different fields and applications, ranging from optoelectronics and high-energy physics to material science and medicine (11–14). One drawback of graphene is its low solubility in both organic and aqueous solvents. For this reason, for biomedical applications, hydrophilic graphene derivatives have been prevailingly used and tested. One among them is graphene oxide (GO). This hydrophilic graphene derivative has been particularly investigated due to its hydrophilicity and low tendency to form aggregates, and therefore its high capacity to homogeneously disperse in water. It is easily produced from cheap graphite via Hummer's oxidative exfoliation (15).

Recently, GO has been reported to exhibit strong antibacterial activity toward both Gram-positive and Gram-negative bacteria (16). To the best of our knowledge, no report is currently available concerning GO effects on biofilms, both in formation and mature, of clinical chronic wound microbial isolates.

Hence, the aim of this work was to investigate the *in vitro* antimicrobial and antibiofilm efficacy of GO against representative wound pathogens, namely, *S. aureus*, *P. aeruginosa*, and *C. albicans*.

RESULTS

Fig. 1 shows the effect of GO at 50 mg/liter on planktonic growth of clinical isolates from chronic wounds, namely, *S. aureus* PECHA 10, *P. aeruginosa* PECHA 4, and *C. albicans* X3. For *S. aureus*, GO significantly reduced bacterial growth after 2 and 24 h compared to that of the respective time controls; no evident ($P > 0.05$) growth increase at 2 and 24 h in respect to the GO $t = 0$ detection was recorded, displaying a clear bacteriostatic effect. For *P. aeruginosa*, after a significant slowdown in the bacterial growth at 2 h of treatment, no significant reduction was recorded at 24 h compared to growth of the respective time controls. The bacteriostatic effect of GO was detected for *P. aeruginosa* after 2 h, compared to the GO $t = 0$ value. *Candida albicans* showed a significant growth reduction after 24 h of treatment with GO in respect to the time control.

Figure 2A and B report the antibiofilm effect of GO on biofilm, both in formation and mature, respectively. For biofilm formation in the presence of GO, a significant reduction of biomass on polystyrene surfaces was recorded for each detected microorganism (Fig. 2A, upper). The representative images in Fig. 2A show the corresponding wells of control and GO, highlighting the visible and clear inhibition of biofilm formation for each strain in the presence of GO. This effect was confirmed by the enumeration of viable and cultivable cells compared to untreated samples (Fig. 2A, lower). The most significant effect was detected for *S. aureus*, with a reduction from 8.63 $\pm$ 0.09 to 6.89 $\pm$ 0.09 $\log_{10}$ CFU/ml. A combined effect of GO can be hypothesized, namely, inhibition of microbial growth and interference with microbial adhesion.

For mature biofilm, GO was able to significantly reduce the produced biomass for all strains, inducing the detachment of cells from the wells, as detectable in the corresponding images (Fig. 2B, upper). An important reduction of the $\log_{10}$ CFU/ml count of mature biofilms was observed after treatment with GO (Fig. 2B, lower). With respect to the controls, all produced biofilms underwent a general detachment from the wells, suggesting a possible GO capability to penetrate into the polymeric matrix of biofilm and to destroy its tridimensional structure.

Subsequently, microscope observations were employed to evaluate cellular changes after treatment with GO.

Figure 3 shows representative images after Gram staining by optical microscopy and

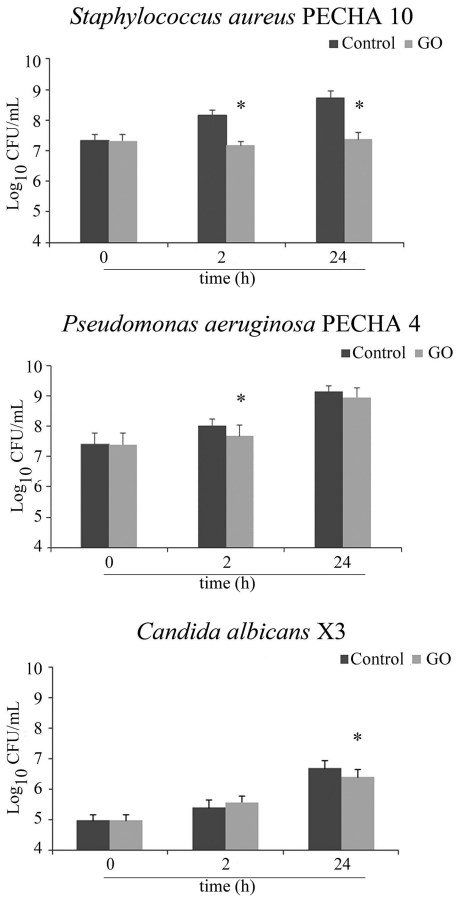

FIG 1 Effect of graphene oxide (GO) at 50 mg/liter on planktonic growth of *Staphylococcus aureus* PECHA 10, *Pseudomonas aeruginosa* PECHA 4, and *Candida albicans* X3 in time. Asterisks indicate the significance ($P < 0.01$) of the difference between the samples treated with GO and the respective time controls.

images recorded by using atomic force microscopy (AFM). After treatment with GO for 24 h, Gram staining showed that GO was capable of trapping *S. aureus* and *C. albicans* (Fig. 3, arrows). This effect was confirmed by AFM images, where isolated and barely flattened cells wrapped with a thin layer of GO (Fig. 3, arrows) were detected. The trapping effect of GO was not detected for *P. aeruginosa* (Fig. 3, asterisks).

Figure 4 demonstrates that all of the investigated microorganisms are characterized by a relatively negative zeta potential. The particularly high value for *S. aureus* could be related to the presence of teichoic acid in the outer surface of the bacterium. Zeta potential measurements were included to show that the interactions between GO and bacteria are not only electrostatic, but that they are linked to stronger covalent interactions.

DISCUSSION

Graphene is a material with potential applications in many fields (17–19). In particular, GO has received increasing attention in biomedical fields for its antimicrobial effect (20–23).

Lot of studies investigated the GO effect after 2 h of contact (20, 23); in this work we wanted to evaluate the effect of GO over time, to study both immediate and tardive effects on microbial cells (after 2 and 24 h). Results showed an immediate and tardive effect against *S. aureus* and only an immediate effect against *P. aeruginosa*, with a significant reduction of planktonic growth compared to the respective time controls. In the presence of GO, no increase in the *S. aureus* planktonic population was recorded at either detected time, whereas for *P. aeruginosa* this bacteriostatic effect was observed only at 2 h.

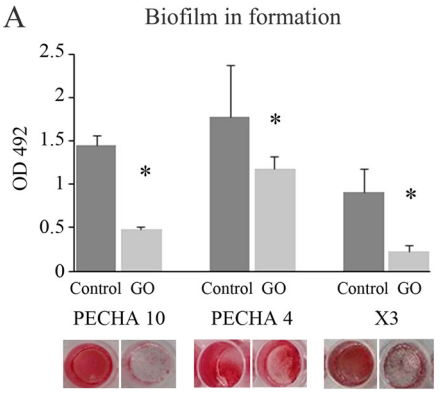

Biofilm in formation (Log_{10}CFU/mL ± sd)

	Control	GO
S. aureus PECHA 10	8.63 ± 0.09	6.89 ± 0.09
P. aeruginosa PECHA 4	8.51 ± 0.07	7.64 ± 0.15
C. albicans X3	7.58 ± 0.17	6.55 ± 0.12

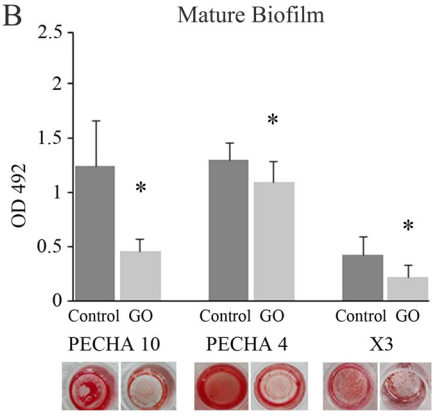

Mature Biofilm (Log_{10}CFU/mL ± sd)

	Control	GO
S. aureus PECHA 10	6.84 ± 0.13	5.89 ± 0.05
P. aeruginosa PECHA 4	9.24 ± 0.02	8.73 ± 0.16
C. albicans X3	8.16 ± 0.21	7.22 ± 0.22

FIG 2 Effect of graphene oxide (GO) at 50 mg/liter on sessile phase of *Staphylococcus aureus* PECHA 10, *Pseudomonas aeruginosa* PECHA 4, and *Candida albicans* X3. (A) Activity of GO on biofilm in formation. (B) Activity of GO on mature biofilm. (A and B, upper) Biomass quantification and representative images before safranin solubilization compared to those of the respective controls. (A and B, lower) CFU counts (log_{10} CFU/ml) compared to those of the respective controls.

As previously reported for some Gram-negative and Gram-positive bacteria (24–28), we observed a weak antibacterial activity against *P. aeruginosa* and a greater loss of viability over time for *S. aureus*. The recorded inhibition of microbial growth is probably due to the complete wrapping of single bacterial cells by GO and the consequent interruption of its metabolic activity (i.e., discontinuance of nutrient metabolism). As evidenced by optical microscopy and AFM measurements, the cells still maintained their spherical shape and cell integrity, no sign of membrane damage could be envisaged, and the deflation of the cells observed by measuring their thickness by AFM high profile is not statistically significant. It is very likely that GO wraps the cells up by interacting with the peptidoglycan layer. As a matter of fact, the peptidoglycan consists of sugars, formed of alternating residues of β1-4-linked *N*-acetylglucosamine (NAG) and *N*-acetylmuramic acid (NAM), and amino acids, and the free amino groups of these

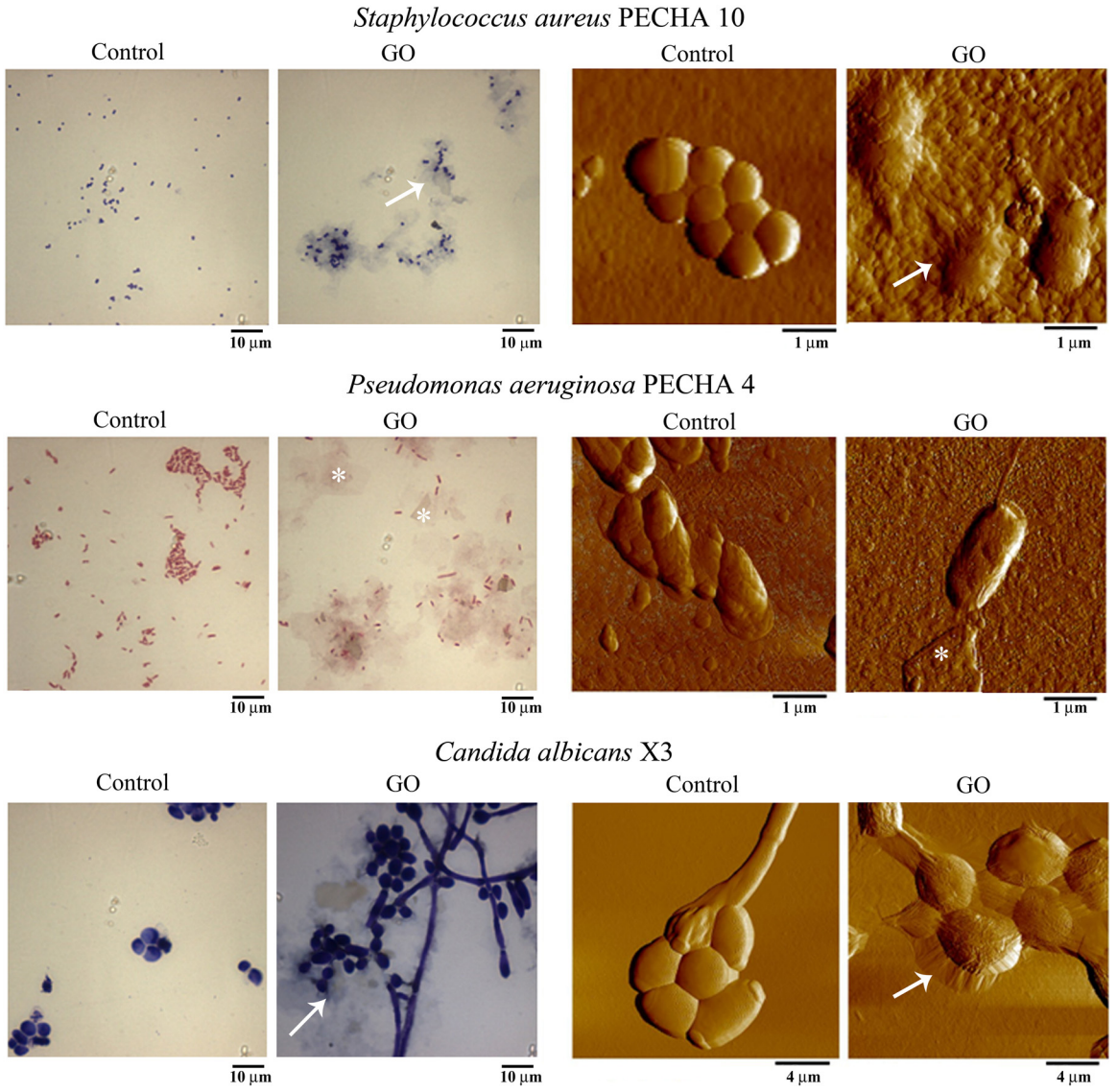

FIG 3 Effect of graphene oxide (GO) at 50 mg/liter on planktonic phase of *Staphylococcus aureus* PECHA 10, *Pseudomonas aeruginosa* PECHA 4, and *Candida albicans* X3. Representative images of control samples and those treated with GO, obtained with Gram staining (columns on the left) and AFM (columns on the right). Arrows indicate GO wrapping microorganisms. Asterisks indicate the GO layer.

molecules can easily form amide linkages with GO (29). The consequent isolation of the bacterium from the growth medium simply reduces its duplication rate. It may appear anomalous that GO, characterized by a relatively negative zeta potential, interacts with the highly negative surface charge of Gram-positive. Nevertheless, covalent bonds among carboxylic groups and reactive epoxide moieties of GO and amine of peptidoglycan and amino acids, as well as hydrogen bond interactions between carbonyl and hydroxyl groups of peptidoglycan, teichoic acid, and GO, easily counterbalance electrostatic interactions (29, 30). These interactions are confirmed by AFM analyses, which evidenced how *S. aureus* is overlaid by GO. On the other hand, the interactions of GO with *P. aeruginosa* are strongly depressed, and AFM showed the low tendency of *P. aeruginosa* to establish a contact with the GO flake. This evidence is in perfect agreement with recently published force spectroscopy measurements that demonstrated that the physical interactions between GO and *Escherichia coli* cells are prevailingly repulsive (30). Indeed, Akhavan et al. (16) suggested that the outer cell membranes of Gram-negative bacteria protect them from GO damage.

The suggested effect of GO on the bacteria investigated here is thus different from

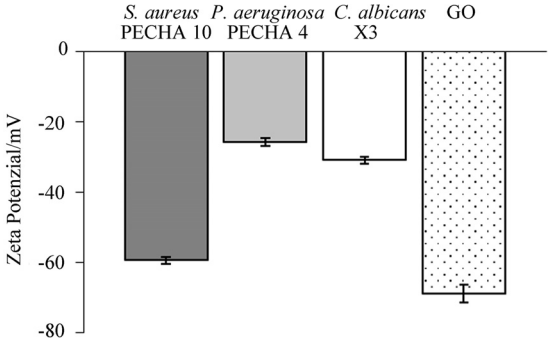

FIG 4 Zeta potential values for *Staphylococcus aureus* PECHA 10, *Pseudomonas aeruginosa* PECHA 4, *Candida albicans* X3, and GO in milliQ water.

that described in literature, where flattened and completely disrupted cells were evidenced (27), but it is in line with previous work (31), where bacteria were demonstrated to be trapped within the aggregated sheets of graphene and could not proliferate in the culture medium. This difference is probably due to the different size of GO flakes. Those investigated in the present paper are micrometer-sized GO (dynamic laser light scattering [DLS] measurements evidenced a diameter of 830 $\pm$ 50 nm, thus confirming the producer characterization) and they are recognized to be too big to enter the membrane and puncture it (16, 28).

For *C. albicans*, no relevant effect was recorded at 2 h of treatment, but a significant reduction in growth was observed after 24 h of incubation. To our knowledge, no information about the effect of GO on yeasts is available. For the first time, we tested GO against *C. albicans* cultures isolated from wound chronic ulcers. The tardive effect of GO is probably due to the lower growth rate of the yeast. The same mechanisms observed for *S. aureus* can be hypothesized for *C. albicans*; that is, GO entraps yeasts within the sheets and disconnects them from the environment, as shown by AFM images. Indeed, the cell wall of *C. albicans* is in part formed by 2 to 4% chitin (NAG) and 80 to 90% glucans and mannans.

C. albicans is a dimorphic opportunistic fungus that is able to invade wounds, contributing to interference with normal wound healing (8). The yeast form plays a key role in the dissemination and systemic infection (32), and the hyphal morphology is important for biofilm formation and is involved in the establishment and maintenance of the infection. In this work, we observed that the addition of GO induces a sustained hyphal morphology. Despite the fact that much remains unclear and additional studies are needed, it is plausible that GO affects the cell separation process, inducing the polarized growth of hyphae, as shown by microscopic observations.

Chronic wounds are an increasing problem characterized by an abnormal wound healing process that is in part due to microbial biofilm formation. Fazli et al. (5) demonstrated a nonrandom distribution of *P. aeruginosa* and *S. aureus* in wounds. Bacteria are present as large aggregates in the wound bed, and *S. aureus* aggregates are located at the wound surface, whereas the *P. aeruginosa* clusters are in the deeper part of the wound bed. The capability of GO to affect the superficial staphylococcal barrier could allow antimicrobials to reach the deeper sites and affect the basal microbial part.

The microbial biofilm mode of growth allows microbes to protect themselves against the host immune system and antimicrobial agents, making biofilm-related infections difficult to treat and eradicate. We tested the effect of GO on biofilm formation and mature biofilm, highlighting the capability of GO to hinder microbial adhesion and penetrate the biofilm matrix.

This effect is likely due to the strong capacity of GO to solubilize in different polymeric environments through specific interactions of polymers and proteins given its wide and carbon rich but hydrophilic surface (18, 33, 34); i.e., hydrogen bond interactions between carbonyl and hydroxyl groups abundant in polysaccharides and

GO and π-π interactions between the DNA and RNA bases and graphenic domains in GO. These interactions disfavor microorganisms aggregation (28) and adhesion on the surfaces (35). In particular, the antibiofilm effect is sustained by the synergic effects of the reduction of microbial growth and by the inhibition of the adhesion of microorganisms to each other and on the surfaces.

The antibacterial and antibiofilm properties of GO against chronic wound microorganisms make it an interesting candidate to incorporate into wound bandages to treat and/or prevent microbial infections.

MATERIALS AND METHODS

Microbial cultures. *Staphylococcus aureus* PECHA 10, *P. aeruginosa* PECHA 4, and *C. albicans* X3 clinical isolates, obtained from the private collection of the Bacteriological Laboratories of the Department of Pharmacy, University "G. d'Annunzio" Chieti-Pescara, were used in this study. These three microorganisms were isolated from the wounds of patients with chronic venous leg ulcers and cultured on mannitol salt agar, cetrimide agar, and Sabouraud dextrose (SAB; Oxoid, Milan, Italy) agar, respectively. For the experiments, bacteria were cultured in Trypticase soy broth (TSB; Oxoid) and incubated at 37°C overnight in aerobic condition. Cultures were refreshed for 2 h at 37°C in an orbital shaker in aerobic condition and standardized at $\sim 5 \times 10^7$ CFU/ml in TSB diluted 1:5 in phosphate-buffered saline (PBS). Previous analysis demonstrated that TSB 1:5 did not interfere with GO characterization (data not shown). Fresh colonies of *C. albicans* grown on SAB agar were used to obtain a broth culture at $\sim 5 \times 10^5$ CFU/ml in RPMI 1640 (Sigma-Aldrich, Milan, Italy) plus 2% glucose (36).

Preparation of GO aqueous dispersion. An aqueous solution of 4 g/liter GO (Graphenea, Donostia-San Sebastian, Spain) was diluted in PBS at the elected concentration, bath ultrasonicated for 10 min (37 kHz, 180 W; Elmasonic P60H; Elma), and sterilized for 2 h under a UV lamp (6 W, 50 Hz, 0.17 A; Spectroline EF 160/C FE; Spectronics). The concentration of GO was checked by UV-visible (UV-vis) spectrophotometry at $\lambda_{max} = 230$ nm. Dimensions of GO flakes were measured by using dynamic laser light scattering (DLS) (90Plus/BI-MAS ZetaPlus multi angle particle size analyzer; Brookhaven Instruments Corp.) (21).

Antimicrobial activity. The standardized broth cultures of *S. aureus* PECHA 10, *P. aeruginosa* PECHA 4, and *C. albicans* X3, prepared as indicated above, were incubated with GO at a final concentration of 50 mg/liter in TSB (final dilution 1:10 in PBS) for bacteria and in RPMI 1640 plus 2% glucose (final diluted 1:2 in PBS) for *C. albicans*, at 37°C for 2 and 24 h to evaluate both an immediate and tardive effect. As controls, bacteria were incubated with fresh, diluted TSB (1:10 in PBS) and *C. albicans* was incubated with diluted RPMI 1640 plus 2% glucose (1:2 in PBS). The microbial viability was evaluated at $t = 0$, 2 h, and 24 h by counting the CFU with the Star-Count STC 1000 colony counter (VWR International PBI Srl, Milan, Italy). Briefly, series of 10-fold cell dilutions (100-μl) were spread on Trypticase soy agar (TSA) plates for bacteria and on SAB agar for *C. albicans* and incubated for 24 to 48 h at 37°C. The cell growth inhibition was detected by comparing the colony counts of GO versus those of the respective time control and those of GO versus those of the GO $t = 0$ detection (37).

Graphene oxide effect on biofilm formation. The effect of GO on bacterial and *C. albicans* biofilm formation ability was tested on flat-bottomed polystyrene microtiter plates for (i) biofilm biomass evaluation by the safranin staining method (38) and (ii) the CFU count for the quantification of cultivable cells (37).

Briefly, bacterial cultures were grown overnight in TSB, refreshed, and standardized in TSB 1:5 plus 0.5% (vol/vol) glucose, as described above. Aliquots of 100 μl were dispensed into each well of 96-well flat-bottomed polystyrene microtiter plates treated with collagen, in the presence of 100 μl of GO at final concentration of 50 mg/liter or of 100 μl sterile PBS (control). *Candida albicans* cultures (100-μl), standardized in RPMI 1640 plus 2% glucose as described above, were dispensed into each well of 96-well flat-bottomed polystyrene microtiter plates in the presence of 100 μl of GO at final concentration of 50 mg/liter or of 100 μl PBS (control).

Each well was incubated for 24 h at 37°C; afterward, (i) for the biofilm biomass evaluation, each well was washed twice with sterile PBS, dried, stained for 1 min with 0.1% safranin, and eluted in 200 μl ethanol, and optical density at 492 nm (OD_{492}) was measured by spectrophotometry using an enzyme-linked immunosorbent assay (ELISA) microplate reader (SAFAS, Munich, Germany), and (ii) for the quantification of cultivable cells, each well was washed twice with sterile PBS to remove nonadherent cells and then scraped. The bacterial suspensions were sonicated by an ultrasonic bath (160 W, 220/240 V, 50 to 60 Hz; FALC ultrasonic cleaning instrument; Treviglio, Italy) for 6 min, and the *C. albicans* suspension was vortexed for 3 min with glass beads to disaggregate microbial aggregates. Microscopic observations of live/dead staining (Invitrogen, Milan, Italy) prior to plating confirmed that the microbial suspension consisted of a mixture of single, viable microbial cells (data not shown).

After treatments, each sample was serially diluted (1:10) in PBS and plated on TSA for bacteria and on SAB for *C. albicans* and incubated for 24 to 48 h at 37°C. The cell concentration was calculated as a mean value of all detections and reported as $\log_{10}$ CFU/ml.

Graphene oxide effect on mature biofilm. The effect of GO on bacterial biofilms and *C. albicans* mature biofilm was tested on flat-bottomed polystyrene microtiter plates for (i) biofilm biomass evaluation by safranin staining method (38) and (ii) the CFU count for the quantification of cultivable cells (37).

The overnight bacterial cultures, as described above, were refreshed for 2 h at 37°C in an orbital shaker under aerobic conditions and standardized at $\sim 5 \times 10^7$ CFU/ml in TSB 0.5% (vol/vol) glucose.

Fresh colonies of *C. albicans* grown on SAB agar were used to obtain a broth culture at ~5 × 10^5 CFU/ml in RPMI 1640 (Sigma-Aldrich, Milan, Italy) plus 2% glucose. Microbial standardized cultures were incubated on 96-well flat-bottomed microtiter plates at 37°C for 24 h. Subsequently, the planktonic cells were gently removed, and the wells were washed with sterile PBS and filled with 200 μl of GO solution (50 mg/liter) or with PBS for the control. After incubation for 24 h at 37°C, each well was washed twice with sterile PBS and subjected to (i) biofilm biomass evaluation by the safranin method and (ii) quantification of cultivable cells, as described above.

Preparation of microbial suspension for zeta potential measurements. Microbial suspensions were prepared as described above. The obtained suspensions were centrifuged (8,000 rpm, 30 min) to pellet the microbial cells before further analysis. For zeta potential measurements, the microbial cell suspensions were prepared by resuspending the cell pellets in MilliQ water. Zeta potential data were obtained by using a ZetaPALS zeta potential analyzer (Brookhaven Instruments Corp.) This measurement was performed in order to investigate how GO interacts with microorganisms (39).

Optical microscopic and atomic force microscopic observations. For the microscopic observations, *S. aureus* PECHA 10, *P. aeruginosa* PECHA 4, and *C. albicans* X3 were treated with GO (50 mg/liter) in TSB (1:10 in PBS) for bacteria and in RPMI 1640 plus 2% glucose (1:2 in PBS) for *C. albicans* and incubated for 24 h at 37°C. For the controls, bacteria were incubated with diluted TSB (1:10 in PBS) and *C. albicans* with diluted RPMI 1640 plus 2% glucose (1:2 in PBS). From each broth culture, 10 μl was Gram-stained and observed microscopically under a Leica 4000 DM microscope (Leica Microsystems S.p.A., Milan, Italy).

Atomic force microscopy (AFM) measurements were performed by using a MultiMode 8 Bruker AFM microscope with a Nanoscope V controller (Bruker, Billerica, MA). A silicon cantilever and an RTESPA-150 tip (spring constant, 5 N/m; resonant frequency 150, kHz) were used in a tapping in air mode. Each broth culture (10-μl), prepared as described above, was placed on a sterile glass square (0.5 × 0.5 cm), air dried, and observed under AFM (40).

Statistical analysis. The statistical significance of differences between controls and experimental groups was evaluated using Student's *t* test. Probability levels of $< 0{\cdot}05$ were considered statistically significant. All data were obtained from three independent experiments performed at least in triplicate.

ACKNOWLEDGMENTS

We thank the student Laura Chiarella for her help during the experiments.

This work was supported by FAR grants held by Luigina Cellini and Mara Di Giulio.

REFERENCES

1. Hannigan GD, Pulos N, Grice EA, Mehta S. 2015. Current concepts and ongoing research in the prevention and treatment of open fracture infections. Adv Wound Care (New Rochelle) 4:59–74. https://doi.org/10.1089/wound.2014.0531.
2. Gottrup F. 2004. A specialized wound healing center concept: importance of a multidisciplinary department structure and surgical treatment facilities in the treatment of chronic wounds. Am J Surg 187:38S–43S. https://doi.org/10.1016/S0002-9610(03)00303-9.
3. Edmonds M. 2012. Body of knowledge around the diabetic foot and limb salvage. J Cardiovasc Surg (Torino) 53:605–606.
4. James GA, Swogger E, Wolcott R, Pulcini ed, Secor P, Sestrich J, Costerton JW, Stewart PS. 2008. Biofilms in chronic wounds. Wound Repair Regen 16:37–44. https://doi.org/10.1111/j.1524-475X.2007.00321.x.
5. Fazli M, Bjarnsholt T, Kirketerp-Møller K, Jørgensen B, Andersen AS, Krogfelt KA, Givskov M, Tolker-Nielsen T. 2009. Nonrandom distribution of *Pseudomonas aeruginosa* and *Staphylococcus aureus* in chronic wounds. J Clin Microbiol 47:4084–4089. https://doi.org/10.1128/JCM.01395-09.
6. DeLeon S, Clinton A, Fowler H, Everett J, Horswill AR, Rumbaugh KP. 2014. Synergistic interactions of *Pseudomonas aeruginosa* and *Staphylococcus aureus* in an *in vitro* wound model. Infect Immun 82:4718–4728. https://doi.org/10.1128/IAI.02198-14.
7. Kalan L, Loesche M, Hodkinson BP, Heilmann K, Ruthel G, Gardner SE, Grice EA. 2016. Redefining the chronic-wound microbiome: fungal communities are prevalent, dynamic, and associated with delayed healing. mBio 7:e01058-16. https://doi.org/10.1128/mBio.01058-16.
8. Chellan G, Shivaprakash S, Karimassery Ramaiyar S, Varma AK, Varma N, Thekkeparambil Sukumaran M, Rohinivilasam Vasukutty J, Bal A, Kumar H. 2010. Spectrum and prevalence of fungi infecting deep tissues of lower-limb wounds in patients with type 2 diabetes. J Clin Microbiol 48:2097–2102. https://doi.org/10.1128/JCM.02035-09.
9. Olsen I. 2015. Biofilm-specific antibiotic tolerance and resistance. Eur J Clin Microbiol Infect Dis 34:877–886. https://doi.org/10.1007/s10096-015-2323-z.
10. Novoselov K, Geim A, Morozov S, Jiang D, Zhang Y, Dubonos SV, Grigorieva IV, Firsov AA. 2004. Electric field effect in atomically thin carbon films. Science 306:666–669. https://doi.org/10.1126/science.1102896.
11. Xia F, Mueller T, Golizadeh-Mojarad R, Freitag M, Lin YM, Tsang J, Perebeinos V, Avouris P. 2009. Photocurrent imaging and efficient photon detection in a graphene transistor. Nano Lett 9:1039–1044. https://doi.org/10.1021/nl8033812.
12. Novoselov K, Geim AK, Morozov S, Jiang D, Katsnelson MI, Grigorieva IV, Dubonos SV, Firsov AA. 2005. Two-dimensional gas of massless Dirac fermions in graphene. Nature 438:197–200. https://doi.org/10.1038/nature04233.
13. Stampfer C, Schurtenberger E, Molitor F, Güttinger J, Ihn T, Ensslin K. 2008. Tunable graphene single electron transistor. Nano Lett 8:2378–2383. https://doi.org/10.1021/nl801225h.
14. Ettorre V, De Marco P, Zara S, Perrotti V, Scarano A, Di Crescenzo A, Petrini M, Hadad C, Bosco D, Zavane B, Valbonetti L, Spoto G, Iezzi G, Piattelli A, Cataldia A, Fontana A. 2016. *In vitro* and *in vivo* characterization of graphene oxide coated porcine bone granules. Carbon 103:291–298. https://doi.org/10.1016/j.carbon.2016.03.010.
15. Hummers WS, Offeman RE. 1958. Preparation of graphitic oxide. J Am Chem Soc 80:1339–1339. https://doi.org/10.1021/ja01539a017.
16. Akhavan O, Ghaderi E. 2010. Toxicity of graphene and graphene oxide nanowalls against bacteria. ACS Nano 4:5731–5736. https://doi.org/10.1021/nn101390x.
17. Ji H, Sun H, Qu X. 2016. Antibacterial applications of graphene-based nanomaterials: Recent achievements and challenges. Adv Drug Deliv Rev 105:176–189. https://doi.org/10.1016/j.addr.2016.04.009.
18. Mao HY, Laurent S, Chen W, Akhavan O, Imani M, Ashkarran AA, Mahmoudi M. 2013. Graphene: promises, facts, opportunities, and challenges in nanomedicine. Chem Rev 113:3407–3424. https://doi.org/10.1021/cr300335p.
19. Kuila T, Bose S, Mishra AK, Khanra P, Kim NH, Lee JH. 2012. Chemical functionalization of graphene and its applications. Prog Mater Sci 57:1061–1105. https://doi.org/10.1016/j.pmatsci.2012.03.002.
20. Hu W, Peng C, Luo W, Lv M, Li X, Li D, Huang Q, Fan C. 2010. Graphene-

based antibacterial paper. ACS Nano 4:4317–4323. https://doi.org/10.1021/nn101097v.
21. Zappacosta R, Di Giulio M, Ettorre V, Bosco D, Hadad C, Siani G, Di Bartolomeo S, Cataldi A, Cellini L, Fontana A. 2015. Liposome-induced exfoliation of graphite to few-layer graphene dispersion with antibacterial activity. J Mat Chem B 3:6520–6527. https://doi.org/10.1039/C5TB00798D.
22. He J, Zhu X, Qi Z, Wang C, Mao X, Zhu C, He Z, Li M, Tang Z. 2015. Killing dental pathogens using antibacterial graphene oxide. ACS Appl Mater Interfaces 7:5605–5611. https://doi.org/10.1021/acsami.5b01069.
23. Wu X, Tan S, Xing Y, Pu Q, Wu M, Zhao JX. 2017. Graphene oxide as an efficient antimicrobial nanomaterial for eradicating multi-drug resistant bacteria *in vitro* and *in vivo*. Colloids Surf B Biointerfaces 157:1–9. https://doi.org/10.1016/j.colsurfb.2017.05.024.
24. Notley SM, Crawford RJ, Ivanova EP. 2013. Bacterial interaction with graphene particles and surfaces, p 100–118. *In* Aliofkhazraei M (ed), Advances in graphene science. IntechOpen, London, UK.
25. Ruiz ON, Fernando KA, Wang B, Brown NA, Luo PG, McNamara ND, Vangsness M, Sun YP, Bunker CE. 2011. Graphene oxide: a nonspecific enhancer of cellular growth. ACS Nano 5:8100–8107. https://doi.org/10.1021/nn202699t.
26. Sreeprasad TS, Maliyekkal MS, Deepti K, Chaudhari K, Xavier PL, Pradeep T. 2011. Transparent, luminescent, antibacterial and patternable film forming composites of graphene oxide/reduced graphene oxide. ACS Appl Mater Interfaces 3:2643–2654. https://doi.org/10.1021/am200447p.
27. Some S, Ho SM, Dua Hwang PE, Shin YH, Yoo H, Kang JS, Lee DK, Lee H. 2012. Dual functions of highly potent graphene derivatives-poly-L-lysine composites to inhibit bacteria and support human cells. ACS Nano 6:7151–7161. https://doi.org/10.1021/nn302215y.
28. Liu S, Zeng TH, Hofmann Burcombe ME, Wei J, Jiang R, Kong J, Chen Y. 2011. Antibacterial activity of graphite, graphite oxide, graphene oxide and reduced graphene oxide: membrane and oxidative stress. ACS Nano 5:6971–6980. https://doi.org/10.1021/nn202451x.
29. Zuo P-P, Feng H-F, Xu Z-Z, Zhang LF, Zhang YL, Xia W, Zhang WQ. 2013. Fabrication of biocompatible and mechanically reinforced graphene oxide-chitosan nanocomposite films. Chem Cent J 7:39. https://doi.org/10.1186/1752-153X-7-39.
30. Romero-Vargas Castrillon S, Perreault F, Fonseca de Faria A, Elimelech M. 2015. Interaction of graphene oxide with bacterial cell membranes: insights from force spectroscopy. Environ Sci Technol Lett 2:112–117. https://doi.org/10.1021/acs.estlett.5b00066.
31. Mejías Carpio IE, Santos CM, Wei X, Rodrigues DF. 2012. Toxicity of a polymer–graphene oxide composite against bacterial planktonic cells, biofilms, and mammalian cells. Nanoscale 4:4746–4756. https://doi.org/10.1039/c2nr30774j.
32. Heilmann CJ, Sorgo AG, Siliakus AR, Dekker HL, Brul S, de Koster CG, de Koning LJ, Klis FM. 2011. Hyphal induction in the human fungal pathogen *Candida albicans* reveals a characteristic wall protein profile. Microbiology 157:2297–2307. https://doi.org/10.1099/mic.0.049395-0.
33. Kim H, Abdala AA, Macosko CW. 2010. Graphene/polymer nanocomposites. Macromolecules 43:6515–6530. https://doi.org/10.1021/ma100572e.
34. Mu Q, Jiang G, Chen L, Zhou Fourches D, Tropsha A, Yan B. 2014. Chemical basis of interactions between engineered nanoparticles and biological systems. Chem Rev 114:7740–7781. https://doi.org/10.1021/cr400295a.
35. Mahmoudi M, Akhavan O, Ghavami M, Rezaee F, Ghiasic SMA. 2012. Graphene oxide strongly inhibits amyloid beta fibrillation. Nanoscale 4:7322–7325. https://doi.org/10.1039/c2nr31657a.
36. Cataldi V, Di Bartolomeo S, Di Campli E, Nostro A, Cellini L, Di Giulio M. 2015. *In vitro* activity of *Aloe vera* inner gel against microorganisms grown in planktonic and sessile phases. Int J Immunopathol Pharmacol 28:595–602. https://doi.org/10.1177/0394632015600594.
37. Baffoni M, Bessa LJ, Grande R, Di Giulio M, Mongelli M, Ciarelli A, Cellini L. 2012. Laser irradiation effect on *Staphylococcus aureus* and *Pseudomonas aeruginosa* biofilms isolated from venous leg ulcer. Int Wound J 9:517–524. https://doi.org/10.1111/j.1742-481X.2011.00910.x.
38. Nostro A, Cellini L, Ginestra G, D'Arrigo M, Di Giulio M, Marino A, Blanco AR, Favaloro A, Bisignano G. 2014. Staphylococcal biofilm formation as affected by type acidulant. APMIS 122:648–653. https://doi.org/10.1111/apm.12210.
39. de Kerchove AJ, Elimelech M. 2005. Relevance of electrokinetic theory for "soft" particles to bacterial cells: implications for bacterial adhesion. Langmuir 21:6462–6472. https://doi.org/10.1021/la047049t.
40. Yamashita H, Taoka A, Uchihashi T, Asano T, Ando T, Fukumori Y. 2012. Single-molecule imaging on living bacterial cell surface by high-speed AFM. J Mol Biol 422:300–309. https://doi.org/10.1016/j.jmb.2012.05.018.